Int. j. adv. multidisc. res. stud. 2022; 2(6):737-741

Received: 18-10-2022
Accepted: 28-11-2022

International Journal of Advanced Multidisciplinary Research and Studies

ISSN: 2583-049X

Methane CH_4 concentration measurements in the mid-infrared range utilizing a TDLS spectrometer calibration relation

[1] Ruaa Kahtan Mahmood, [2] Samira A Mahdi, [3] Amal Abd Al-Amir Al Masoudi
[1, 2, 3] Department of Physics, College of Sciences, University of Babylon, Babylon, 51001, Iraq

Corresponding Author: **Ruaa Kahtan Mahmood**

Abstract
The simulation approach of TDLS has been proven in this study to improve spectrometer sensitivity by modifying the wavelength of a DFB tunable laser diode using a sinusoid signal. Because the laser's driving current has been set, the wavelength of the laser diode will shift in tuning limits to around 0.02 nm in the Mid Infrared Area (MIR) region for a poisonous gas Methane CH4.
The sensitivity of TDLS was tested at a constant concentration of 0.5ppb and a constant length of the open path (the distance between the laser source and the retroreflector) of 100m. After writing a MATLAB algorithm to set the correct wavelength in the MIR region, frequency domain measurements were performed to extract the second harmonic as an indication of gas presence. The precise wave length of methane gas in the MIR area is (3290.987nm). It should be noted that for all gas types measured at L = 100 m, the gas concentration ranged from N = 0.05 to 0.5 ppm in 0.2 steps.

Keywords: TDLS, Methane Gas, Wavelength Tuning

1. Introduction

Monitoring and detection of atmospheric gas concentrations has become extremely valuable as a result of global warming and climate change. Despite the fact that the typical background level of methane (CH4) (1.89 ppm) in the earth's atmosphere is nearly 200 times lower than that of CO2 (400 ppm), CH4 contributes 25 times more to the greenhouse effect per mole than CO2 [1, 2]. As a result, rapid, quick, and exact monitoring of trace greenhouse gas of CH4 is critical. Chemical processes [3-6] and optical spectroscopy [7-9] are two methods for detecting methane.

Optical spectroscopy for gas detection is based on the Beer-Lambert rule [10-12], which states that light attenuation is proportional to the effective length of the sample in an absorbing medium and the concentration of absorbing species. According to this theory, the emission wavelength of the narrow-linewidth diode laser is scanned over the target gas absorption line, and due to the advantage of high spectrum resolution, tunable diode laser absorption spectroscopy (TDLAS) has become an effective technique for the rapid and online analysis of gas component concentration [13-22]. The most prevalent TDLAS sensing techniques are direct detection and wavelength modulation spectroscopy [23, 24].

In comparison, wavelength/frequency modulation spectroscopy is less susceptible to the effects of background noise and is better suited for identifying trace gases. Furthermore, modulation spectroscopy is commonly employed for gas detection because to its high signal-to-noise ratio (SNR) [25, 26]. The primary approaches in modulation absorption spectroscopy are wavelength modulation spectroscopy (WMS), frequency modulation spectroscopy (FMS), and two-tone frequency modulation spectroscopy (TTFMS). Because each approach has advantages and disadvantages, they have all been used to detect methane in various situations. Following an introduction to methane absorption characteristics and current advancements in tunable diode lasers (TDLs), this paper presents recent advances in methane detection utilizing modulation spectroscopy. The spherical top of the CH4 molecule belongs to the tetrahedral point family.

It has four basic vibration modes, which are as follows: ν1 = 2913 cm-1, ν 2 = 1533.3 cm-1, ν3= 3018.9 cm-1, and ν4 = 1305.9 cm-1 [27]. The two bending vibrations are 2 (asymmetric) and 4 (symmetric), whereas the two stretching vibrations are 1 (symmetric) and 3 (asymmetric) [28]. The gap between successive resonances is approximately 1500 cm-1 [29]. The 23 band near 1670 nm and the ν2 + 2ν3 band near 1300 nm are primary overtone rotational-vibrational combination bands in the near-infrared region (1100-1800 nm) [30].

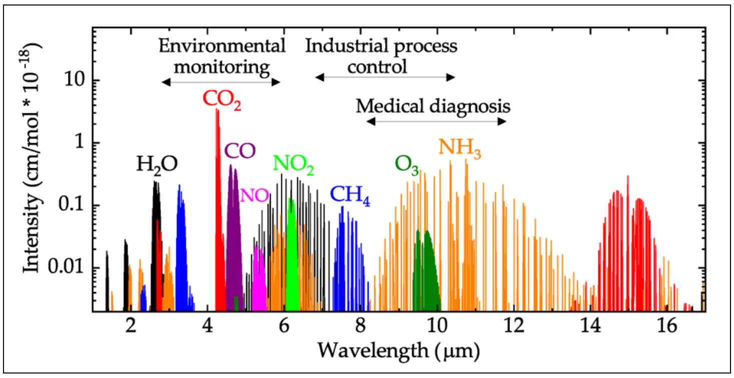

Fig 1: describe MID-infrared absorption spectra of gases [31]

2. Theory (Simulations)

The Beer-Lambert Law underpins models of light absorption by gases. [32]:

$$I = I_o e^{-\beta\sigma NL} \tag{1}$$

Where Io is the fundamental incident intensity of IR laser light received by the photodiode in the absence of gas. The incident intensity was modulated using a sinusoidal waveform, as shown in Eq. 2.

$$I_o = [(i_{offset} - i_{th}) + a \sin\ (2\pi f_o t)] \frac{\delta}{area} \tag{2}$$

where $i_{offset} = 99$ mA is the DC offset; $i_{th} = 19$ mA is the threshold current; $a = 42$ mA is the amplitude of the sine wave; $f_o = 500$ Hz is the modulation frequency; $\delta = 0.2055$ mW/mA is the differential efficiency (the direct relation constant that convert the laser current to the laser power); $area = 3.1$ mm2 is the active area of the photodiode. A narrow bandwidth beam of the laser light was generated and swept through the absorption peak of methane, carbon monoxide gases.

Depending on the weather conditions in the Martian atmosphere, the pressure is only a few millibars, with a mean pressure of roughly 730 Pa = 7. 3 millibar [32]. Doppler broadening dominates and the line-shape of the absorption cross-section σ becomes Gaussian, as shown in Eq. 3.

$$\sigma = C\, e^{-\frac{(w_o + a\ \gamma \sin\ (2\pi f_o\ t) - w_p)^2}{2\varepsilon^2}} \tag{3}$$

If we substitute Eq. (3-2) and Eq. (3-3) in Eq. (4-1) we get:

$$I = [(i_{offset} - i_{th}) + a \sin\ (2\pi f_{mod}\ t)] \frac{\delta}{area} e^{-\beta NLC\, e^{-\frac{(w_o + a\ \gamma \sin(2\pi f_{mod} t) - w_p)^2}{2\varepsilon^2}}} \tag{4}$$

I_0 and I (mW/mm2) are the intensity of incident light and transmitted light, respectively; β is a factor to convert the unit from ppm to cm-3 as follows [33]

3. β Factor Calculation for Methane GAS

$\beta = 1\,ppm = \frac{1mg}{L} = \frac{10^{-3}\,g}{10^3\,M\,cm^3}$, where M is the molecular weight of methane gas, so $c = \frac{10^{-6}\,g}{\frac{16.043g}{mol}cm^3} = 0.0624 \times \frac{10^{-6}\,mol}{cm^3} \times N_A$, NA is the Avogadro number (cm-3/ppm), As a result, $\beta = 0.0624 \times \frac{10^{-3}\,mol}{cm^3} \times 6.022 \times 10^{20} \frac{1}{mol} = 0.365 \times \frac{10^{-3}}{cm^3} \times 10^{20} = 0.365E17$, and; N (parts per million) is the gas concentration; and $L = 100$ m is the light path length through the gas. In Eq. (4), C = 1E-20 cm2 is the cross-section area of the absorption peak of methane gas and its variance $\varepsilon = 0.1$ nm over the wavelength range which appears in the term of $(w_o + a\ \gamma \sin(2\pi f_o\ t) - w_p)$. $w_o = 3290$ nm in mid IR is the initial value of the scanning wavelength of the diode laser; $a\ \gamma \sin(2\pi f_o\ t)$ is the AC current waveform used to adjust the wavelength of emitted light from the laser, with $a = 42$ mA is the amplitude of the sine wave; $\gamma = 0.01$ nm/mA is a modulation factor; fo = 500 Hz is the modulation frequency; t is time in seconds; and FWHM= 0.07 in MIR [34] and $w_p = 3291.6$ nm [35] is the peak value of the absorption spectrum of methane gas in MIR region [36].

4. Methane gas absorption peak in the MIR spectral region

Fig 2 shows the absorption signal of methane gas at tuning current of laser diode (79.90 mA) and wavelength (3290.987 nm). Because the frequency of the light wave matches the vibrational frequencies of the methane gas at this wavelength, the absorption peak is placed exactly in the middle of the sine wave, meaning that the gas has absorbed the whole energy of the sine wave. The concentration of methane gas has been set at 0.5 ppb, and the length of the open path spectrometer has been set at 100m.

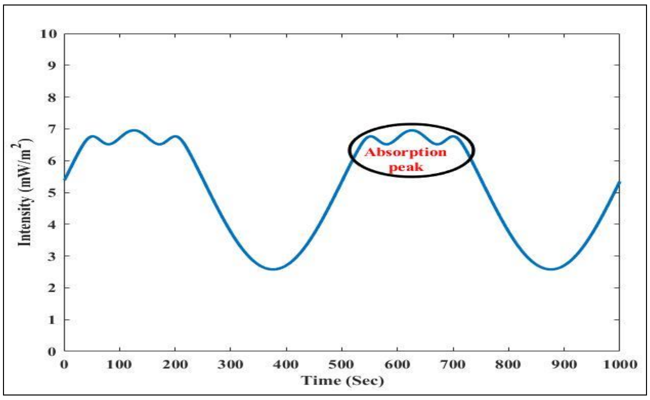

Fig 2: The absorption peak of methane gas in mid infrared region at tuning current of laser diode (79.90mA) and the wavelength (3290.987 nm).

In comparison to Fig 3, there is no absorption signal in the time domain. Because the wavelength of the laser diode does not match the frequencies of the vibrational energy states that can absorb laser light energy.

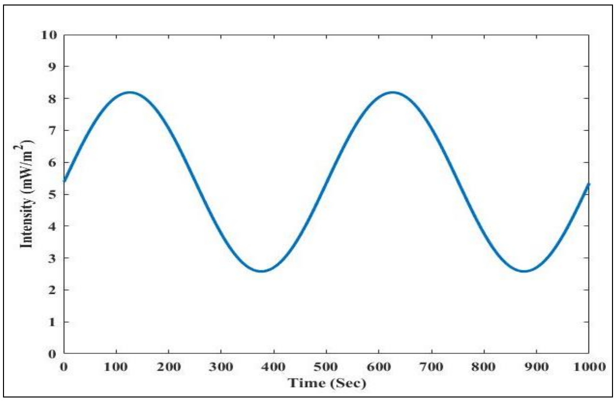

Fig 3: Absence of methane gas in mid infrared region absorption peak at tuning current of laser diode (81.31 mA) and wave length (3291.001 nm)

The second harmonic was extracted as a gas presence indicator using MATLAB code and a fast Fourier transformation (FFT). Fig 4 depicts the fast Fourier Transform (FFT) chart for the time domain data shown in figure. When the fundamental frequency is 500 Hz and the second harmonic is 1000 Hz, the value of the second harmonic appears to be significant (0.18 mW/m2), implying that most of the light energy has been absorbed.

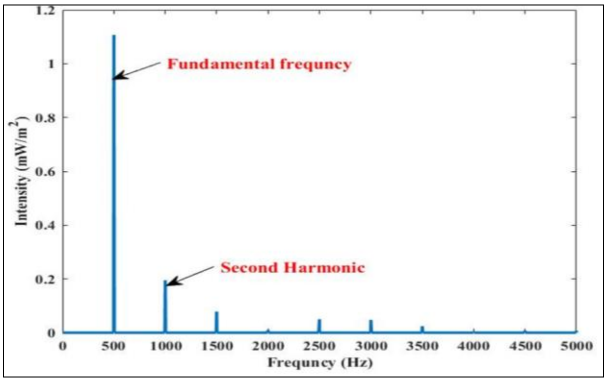

Fig 4: Fundamental frequency of methane gas in mid infrared region at 500 Hz and the absorption peak at 1000 Hz

Fig 5 shows the fundamental frequency and the value of the second harmonic. When the wavelength value is a little off from the desired wavelength value, the second harmonic appears to have been reduced (that is, there is no absorption peak for the methane gas in the mid infrared region).

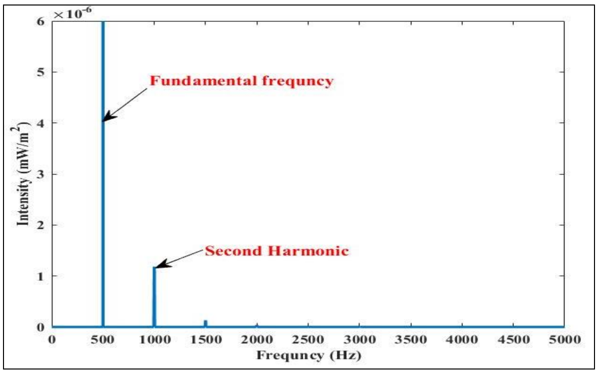

Fig 5: Fundamental frequency of methane gas in mid infrared region at 500 Hz and the amount of the second harmonic reached about zero at 1000Hz

Using a MATLAB code, the amount at the operating current of a laser diode (LD) that may generate a maximum second harmonic value was calculated, and it was discovered that the relationship has a maximum peak and a minimum valley at current values of 79.90 mA and 81.31 mA, respectively, as shown in fig 6.

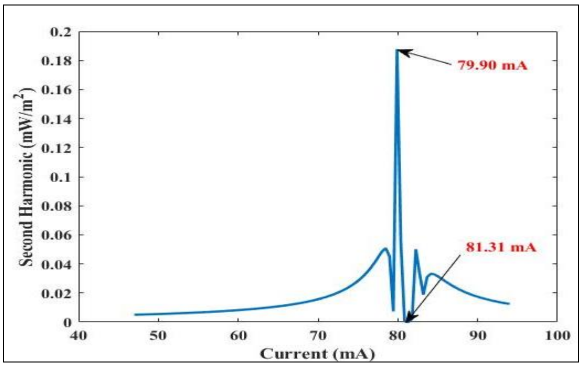

Fig 6: The variation of the second harmonic with the tuning current of methane gas in mid infrared region

The spectrum wavelength was then adjusted in 0.02 nm increments to increase the sensitivity of the tunable diode spectrometer (TDLS). That was the fundamental goal of this endeavor. According to MATLAB code, the relationship has a maximum peak and a minimum valley at wavelengths of 3290.987 nm and 3291.001 nm in the mid infrared, respectively as shown in fig 7.

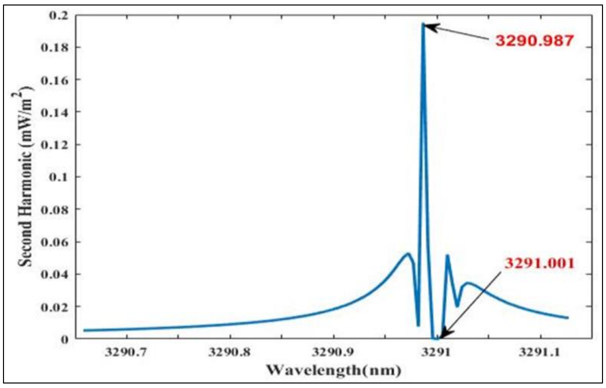

Fig 7: The wavelength spectrum of methane gas in mid infrared region has a one peak at (3290.987 nm) in the mid infrared

Fig 8 displays the relationship between the second harmonic and gas concentration at the needed value of the laser diode produced current and at the right wavelength (3290.987 nm). The connection appears to be linear, and the gas concentration's minimum value was (0.05 ppb).

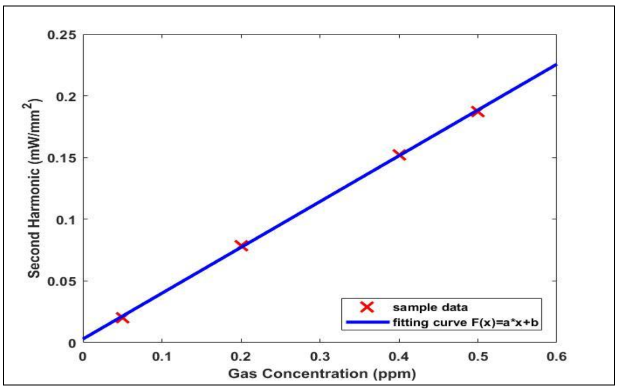

Fig 8: Relation between second harmonic and gas concentration of methane gas in mid infrared region

5. Conclusions

The TDLS modeling approach was used in this study to improve the sensitivity of the spectrometer by changing the wavelength of a DFB tunable laser diode using a sinusoid signal. Because the laser's driving current has been tweaked, the wavelength of the laser diode will shift in tuning limits to around 0.02 nm in the NIR region. This was done to test the sensitivity of the TDLS spectrometer in these spectrum frequency regions. The simulated measurements of the CH4 gas indicated the same minimum gas concentration but at different wavelengths of the DFB tunable laser diode. Whereas in the NIR zone, the precise wavelength was 3290.987nm and the drive was around 79.90 mA.

6. References

1. Rodhe H. A comparison of the contribution of various gases to the greenhouse effect. Science. 1990; 248(4960):1217-1219.
2. Liu K, Wang L, Tan T, Wang G, Zhang W, Chen W, Gao X. Highly sensitive detection of methane by near-infrared laser absorption spectroscopy using a compact dense-pattern multipass cell. Sensors and Actuators B: Chemical. 2015; 220:1000-1005.
3. Karpov EE, Karpov EF, Suchkov A, Mironov S, Baranov A, Sleptsov V, Calliari L. Energy efficient planar catalytic sensor for methane measurement. Sensors and Actuators A: Physical. 2013; 194:176-180.
4. Nagai D, Nishibori M, Itoh T, Kawabe T, Sato K, Shin W. Ppm level methane detection using micro-thermoelectric gas sensors with Pd/Al2O3 combustion catalyst films. Sensors and Actuators B: Chemical. 2015; 206:488-494.
5. Suzuki T, Kunihara K, Kobayashi M, Tabata S, Higaki K, Ohnishi H. A micromachined gas sensor based on a catalytic thick film/SnO2 thin film bilayer and thin film heater: Part 1: CH4 sensing. Sensors and Actuators B: Chemical. 2005; 109(2):185-189.
6. Van der Laan S, Neubert REM, Meijer HAJ. A single gas chromatograph for accurate atmospheric mixing ratio measurements of CO 2, CH 4, N 2 O, SF 6 and CO. Atmospheric Measurement Techniques. 2009; 2(2):549-559.
7. Liu D, Fu S, Tang M, Shum P, Liu D. Comb filter-based fiber-optic methane sensor system with mitigation of cross gas sensitivity. Journal of lightwave technology. 2012; 30(19):3103-3109.
8. Lin H, Liang Z, Li E, Yang M, Zhai B. Analysis and design of an improved light interference methane sensor. In 11th IEEE International Conference on Control & Automation (ICCA). IEEE, June 2014, 404-409.
9. Ma Y, He Y, Tong Y, Yu X, Tittel FK. Quartz-tuning-fork enhanced photothermal spectroscopy for ultra-high sensitive trace gas detection. Optics express. 2018; 26(24):32103-32110.
10. Leigh RJ, Corlett GK, Friess U, Monks PS. Concurrent multiaxis differential optical absorption spectroscopy system for the measurement of tropospheric nitrogen dioxide. Applied Optics. 2006; 45(28):7504-7518.
11. Rustgi OP. Absorption cross sections of argon and methane between 600 and 170 Å. JOSA. 1964; 54(4):464-466.
12. Swinehart DF. The beer-lambert law. Journal of chemical education. 1962; 39(7):333.
13. Kireev SV, Shnyrev SL. On-line monitoring of odorant in natural gas mixtures of different composition by the infrared absorption spectroscopy method. Laser Physics Letters. 2018; 15(3):035705.
14. Wenxue Z, Chuantao Z, Dan Y, Shuo Y, Peipei D, Yiding W. Development of a mid-infrared interband cascade laser methane sensor. Acta Optica Sinica. 2018; 38(3):0328013.
15. Willer U, Saraji M, Khorsandi A, Geiser P, Schade W. Near-and mid-infrared laser monitoring of industrial processes, environment and security applications. Optics and Lasers in Engineering. 2006; 44(7):699-710.
16. Mappé I, Joly L, Durry G, Thomas X, Decarpenterie T, Cousin J, *et al*. A quantum cascade laser absorption spectrometer devoted to the in-situ measurement of atmospheric N2O and CH4 emission fluxes. Review of scientific instruments. 2013; 84(2):023103.
17. Crosson E. A cavity ring-down analyzer for measuring atmospheric levels of methane, carbon dioxide, and water vapor. Applied Physics B. 2008; 92(3):403-408.
18. Berman ES, Fladeland M, Liem J, Kolyer R, Gupta M. Greenhouse gas analyzer for measurements of carbon dioxide, methane, and water vapor aboard an unmanned aerial vehicle. Sensors and Actuators B: Chemical. 2012; 169:128-135.
19. Grossel A, Zeninari V, Parvitte B, Joly L, Courtois D. Optimization of a compact photoacoustic quantum cascade laser spectrometer for atmospheric flux measurements: Application to the detection of methane and nitrous oxide. Applied Physics B. 2007; 88(3):483-492.
20. Schiff HI, Mackay GI, Bechara J. The use of tunable diode laser absorption spectroscopy for atmospheric measurements. Research on chemical intermediates. 1994; 20(3):525-556.
21. Kamieniak J, Randviir EP, Banks CE. The latest developments in the analytical sensing of methane. TrAC Trends in Analytical Chemistry. 2015; 73:146-157.
22. He Y, Ma Y, Tong Y, Yu X, Tittel FK. Ultra-high sensitive light-induced thermoelastic spectroscopy sensor with a high Q-factor quartz tuning fork and a multipass cell. Optics Letters. 2019; 44(8):1904-1907.
23. Behera A, Wang A. Calibration-free wavelength modulation spectroscopy: Symmetry approach and residual amplitude modulation normalization. Applied optics. 2016; 55(16):4446-4455.
24. Bomse DS, Stanton AC, Silver JA. Frequency modulation and wavelength modulation spectroscopies: Comparison of experimental methods using a lead-salt diode laser. Applied optics. 1992; 31(6):718-731.
25. Rojas D, Ljung P, Axner O. An investigation of the 2f—wavelength modulation technique for detection of atoms under optically thin as well as thick conditions. Spectrochimica Acta Part B: Atomic Spectroscopy. 1997; 52(11):1663-1686.
26. Williams RM, Kelly JF, Sharpe SW, Hartman JS, Gmachl CF, Capasso F, *et al*. Spectral and modulation performance of quantum cascade lasers with application to remote sensing. In Application of Tunable Diode and Other Infrared Sources for Atmospheric Studies and Industrial Processing Monitoring II. 1999; 3758:11-22. SPIE.
27. Chan K, Ito H, Inaba H. Absorption Measurement of ν

2+ 2ν 3 band of CH 4 at 1.33 μm Using an InGaAsP Light Emitting Diode. Applied optics. 1983; 22(23):3802-3804.

28. Schilt S, Besson JP, Thévenaz L. Near-infrared laser photoacoustic detection of methane: The impact of molecular relaxation. Applied Physics B. 2006; 82(2):319-328.
29. Shemshad J, Aminossadati SM, Kizil MS. A review of developments in near infrared methane detection based on tunable diode laser. Sensors and Actuators B: Chemical, 171, 77-92.30. Wang, F., Jia, S., Wang, Y., & Tang, Z. (2019). Recent developments in modulation spectroscopy for methane detection based on tunable diode laser. Applied sciences. 2012; 9(14):2816.
30. Gordon IE, Rothman LS, Hargreaves RJ, Hashemi R, Karlovets EV, Skinner FM, *et al*. The HITRAN2020 molecular spectroscopic database. Journal of quantitative spectroscopy and radiative transfer. 2022; 277:107949.
31. Mahdi SA. An investigation of electro-optical 1/f noise reduction in an open-path tunable diode laser spectrometer (Doctoral dissertation, University of Arkansas at Little Rock), 2013.
32. Mahmood RK, Mehdi SA. A simulation process of tunable open path diode laser spectrometer to detect a carbon monoxide gas in NIR region. In IOP Conference Series: Earth and Environmental Science. IOP Publishing. 2022; 961(1):012081.
33. Milton Filho B, da Silva MG, Sthel MS, Schramm DU, Vargas H, Miklós A, *et al*. Ammonia detection by using quantum-cascade laser photoacoustic spectroscopy. Applied optics. 2006; 45(20):4966-4971.
34. Seiter M, Sigrist MW. On-line multicomponent trace-gas analysis with a broadly tunable pulsed difference-frequency laser spectrometer. Applied optics. 1999; 38(21):4691-4698.